Kinetic and Structural Characteristics of the Inhibition of Enoyl (Acyl Carrier Protein) Reductase by Triclosan‡

Walter H. J. Ward,* Geoffrey A. Holdgate, Siân Rowsell, Estelle G. McLean, Richard A. Pauptit, Edward Clayton, Wright W. Nichols, Jeremy G. Colls, Claire A. Minshull, David A. Jude, Anil Mistry, David Timms, Roger Camble, Neil J. Hales, Carolyn J. Britton, and Ian W. F. Taylor

AstraZeneca, Mereside, Alderley Park, Macclesfield, Cheshire, SK10 4TG, U.K.

Received April 2, 1999; Revised Manuscript Received July 14, 1999

ABSTRACT: Triclosan is used widely as an antibacterial agent in dermatological products, mouthwashes, and toothpastes. Recent studies imply that antibacterial activity results from binding to enoyl (acyl carrier protein) reductase (EACPR, EC 1.3.1.9). We first recognized the ability of triclosan to inhibit EACPR from *Escherichia coli* in a high throughput screen where the enzyme and test compound were preincubated with NAD^+, which is a product of the reaction. The concentration of triclosan required for 50% inhibition approximates to 50% of the enzyme concentration, indicating that the free compound is depleted by binding to EACPR. With no preincubation or added NAD^+, the degree of inhibition by 150 nM triclosan increases gradually over several minutes. The onset of inhibition is more rapid when NAD^+ is added. Gel filtration and mass spectrometry show that inhibition by triclosan is reversible. Steady-state assays were designed to avoid depletion of free inhibitor and changes in the degree of inhibition. The results suggest that triclosan binds to E−NAD^+ complex, with a dissociation constant around 20−40 pM. Triclosan follows competitive kinetics with respect to NADH, giving an inhibition constant of 38 pM at zero NADH and saturating NAD^+. Uncompetitive kinetics are observed when NAD^+ is varied, giving an inhibition constant of 22 pM at saturating NAD^+. By following regain of catalytic activity after dilution of EACPR that had been preincubated with triclosan and NAD^+, the rate constant for dissociation of the inhibitor (k_{off}) is measured as 1.9×10^{-4} s^{-1}. The association rate constant (k_{on}) is estimated as 2.6×10^7 s^{-1} M^{-1} by monitoring the onset of inhibition during assays started by addition of EACPR. As expected, the ratio $k_{off}/k_{on} = 7.1$ pM is similar to the inhibition constants from the steady-state studies. The crystal structure of *E. coli* EACPR in a complex with coenzyme and triclosan has been determined at 1.9 Å resolution, showing that this compound binds in a similar site to the diazaborine inhibitors. The high affinity of triclosan appears to be due to structural similarity to a tightly bound intermediate in catalysis.

Biosynthesis of fatty acids involves extension of an S-acyl primer by sequential addition of two carbon units, which is catalyzed in several steps by fatty acid synthetase. Fatty acid synthetases have been classified into two groups (*1*). The type I enzymes occur in vertebrates and certain bacteria, and all of the catalytic functions are performed by residues on one or two polypeptide chains. Type II fatty acid synthetases are found in plants and other bacteria, including *Escherichia coli*. Here, six different enzyme activities are associated with separate polypeptides, one of which is enoyl (acyl carrier protein) reductase (EACPR[1], EC 1.3.1.9). This enzyme catalyses NADH (or NADPH)-dependent reduction of the double bond between C2 and C3 of enoyl ACP (*2*−*4*). The homologous enzyme from *Mycobacterium tuberculosis*, InhA, follows a sequential kinetic mechanism, with NADH preferred as the first substrate to bind (*5*). In *E. coli*, EACPR is a homotetramer ($M_r = 4 \times 27\,700$), which is encoded by the *fabI* gene and has extensive sequence homology with enzymes from *M. tuberculosis* and oilseed rape (*Brassica napus*), but not with the portion of the eukaryotic yeast *FAS1* gene product that encodes EACPR function (*3*). In animals, extramitochondrial EACPR activity is due to a flavodoxin-containing component of the $M_r \approx 500\,000$ fatty acid synthetase complex, which is clearly different to the *E. coli* enzyme.

The catalytic activity of EACPR is essential for viability in *E. coli*. Temperature sensitive mutants die in nonisosmotic medium at nonpermissive temperatures (*3*), and a family of antibacterial agents, the diazaborines, inhibit EACPR by forming a covalent bond with enzyme-bound NAD^+ (*6*, *7*). InhA is the target for indirect inhibition by isoniazid during therapy for tuberculosis. A metabolite of this drug forms a

‡ Coordinates deposited at the PDB, filename: 1QG6.

* Author for correspondence. Telephone: ++44-1625-515998. Fax: ++44-1625-583074. E-mail: walter.ward@astrazeneca.com.

[1] Abbreviations: *a*, apparent rate constant for dissociation (eq A5); *a*′, rate constant for onset of inhibition (eq A23); ACP, acyl carrier protein; [E_0], total concentration of enzyme binding sites; EACPR, enoyl ACP reductase; IC_{50}, concentration giving 50% inhibition; k_{on}, association rate constant; k_{on}', apparent association rate constant (Scheme A1); k_{off}, dissociation rate constant; k_p, apparent rate constant for product formation; K_i, inhibition constant; K_i', apparent inhibition constant (eq 5); K_{ii}, inhibition constant for intercept on Lineweaver−Burk plots; K_{is}, inhibition constant for slope on Lineweaver−Burk plots; K_{NAD}, dissociation constant for NAD^+; v_0, initial velocity; v_s, steady-state velocity; v_u, uninhibited velocity.

10.1021/bi9907779 CCC: $18.00
Published on Web 08/27/1999

covalent bond with the coenzyme, which has complexed to InhA (*8*, *9*).

Given the essential nature of EACPR activity for survival of bacteria and the structural differences compared to the analogous human enzyme, EACPR is a target in the search for novel antibiotics. Accordingly, AstraZeneca evaluated more than 200 000 compounds as inhibitors of EACPR. The most potent inhibitors were tested for the ability to prevent growth of *E. coli*. The locus of antibacterial activity was investigated using mutants, one of which overproduced EACPR and another (Ser-93→Val), which was resistant to diazaborines. Further experiments monitored rates of fatty acid biosynthesis. Triclosan (5-chloro-2-(2,4-dichlorophenoxy) phenol, Structure 1) emerged from these studies as a

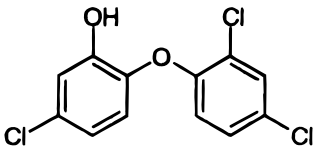

(1)

potent antibacterial agent, which acts by inhibition of EACPR.

Triclosan has been used widely for many years as an antibacterial agent in many products, including antiseptic soaps, toothpastes, mouthwashes, dermatological agents, fabrics, and plastics. McMurry et al. (*10*) recently published that triclosan inhibits fatty acid biosynthesis in *E. coli* and that mutations in, or overexpression of, *fabI* prevent this effect. These observations were confirmed by Heath et al. (*11*), who demonstrated directly that triclosan inhibits the EACPR enzyme. A recent crystal structure at 2.2 Å resolution shows that triclosan can bind to a complex containing EACPR and NAD^+ (*12*). We now describe kinetic and structural characteristics of inhibition of *E. coli* EACPR by triclosan. There is no evidence for formation of a covalent complex, which would be analogous to the diazaborines and the isoniazid metabolite. Accordingly, triclosan differs from these compounds in that it is a reversible inhibitor. The onset of inhibition appears slow, in part because triclosan binds most strongly to a complex containing EACPR and NAD^+, which represents a small proportion of the total enzyme since NAD^+ has a low affinity. The rate of dissociation of triclosan also is slow, giving it an equilibrium dissociation constant around 7−40 pM. The crystal structure of *E. coli* EACPR in a complex with the coenzyme and triclosan has now been determined at 1.9 Å resolution and suggests that the high affinity of the inhibitor is linked with similarity to a tightly bound intermediate in catalysis.

EXPERIMENTAL PROCEDURES

Materials. EACPR was expressed in recombinant *E. coli* BL21 (DE3) pLysS using the pET(hc)10 construct (*13*), which was a generous gift from Dr A. R. Stuitje (Department of Genetics, Institute of Molecular Biological Sciences, Vrije Universiteit, Amsterdam, Netherlands). Cells were grown as a fed batch culture in a 20 L fermentor (B. Braun, Melsungen, Germany), using the following medium: 3 g/L of KH_2PO_4, 6 g/L of Na_2HPO_4, 0.5 g/L of NaCl, 2 g/L of casein hydrolysate, 10 g/L of $(NH_4)_2SO_4$, 35 g/L of glycerol, 20 g/L of yeast extract, 0.5 g/L of $MgSO_4 \cdot 7H_2O$, 30 mg/L of $CaCl_2 \cdot 2H_2O$, 8 mg/L of thiamine, 40 mg/L of $FeSO_4$, 20 mg/L of citric acid, 100 mg/L of ampicillin, 34 mg/L of chloramphenicol, pH 6.7. Cells were grown aerobically at 37 °C, to an A_{550} of 20−25, and then expression was induced with 0.5 mM isopropyl β-D-thiogalactopyranoside. Cells were harvested 5 h later by centrifugation (7000 g at 4 °C for 30 min). The enzyme was purified as described by Bergler et al. (*4*), with the following modifications: all steps were conducted in the presence of 1 mM dithiothreitol, the enzyme was eluted from the DEAE-sepharose by a 100−200 mM NaCl linear gradient rather than by a step gradient, and the enzyme-containing fractions were pooled and loaded directly onto the Blue Sepharose without concentration and desalting. The final product was judged to be 95% pure by sodium dodecyl sulfate-polyacrylamide gel electrophoresis, reverse phase HPLC (C2−C18 Pharmacia column, 3−90% (v/v) acetonitrile gradient in 0.1% (v/v) trifluoroacetic acid) and size exclusion HPLC (Pharmacia Superdex 75, 50 mM BisTris pH 6.5, 1 mM dithiothreitol, 150 mM NaCl).

Assay of EACPR Activity. EACPR (approximately 20 nM) was incubated at 25 °C with various concentrations of NADH and crotonoyl CoA and 1% (v/v) dimethylsulfoxide in 50 mM sodium phosphate, pH 7.5. Depletion of NADH was followed by monitoring A_{340} and assuming $\epsilon = 6220\ M^{-1}\ cm^{-1}$.

Assay to Measure Potency of EACPR Inhibitors. Inhibitors were dissolved in dimethylsulfoxide. EACPR (approximately 150 nM) was preincubated for 30 min at room temperature with 255 mM NAD^+ and inhibitor in the presence of 1.82% (v/v) dimethylsulfoxide and 60.6 mM sodium phosphate, pH 7.5. The assay was started by addition of NADH (to 100 μM) and crotonoyl CoA (to 800 μM), which diluted the preincubation by a factor of 1.82, giving 140 μM NAD^+ and 1% (v/v) dimethylsulfoxide in a total volume of 200 μL. The final buffer was 50 mM sodium phosphate, pH 7.5. Depletion of NADH was followed by monitoring A_{340}.

Analysis of Measured Rates. Equations were fitted to data by unweighted nonlinear regression using *GraFit* (*14*). Identification of the most suitable equation was assisted by an *F*-test (*15*), which was used to compare the residual sum of squares obtained after fitting various relationships, as described by Ward et al. (*16*).

During dose−response analysis, enzyme inhibition often is described accurately by the relationship

$$v = v_u/(1 + [I]/K_i') \quad (1)$$

where v_u is the unihibited rate, K_i' is the apparent inhibition constant. This rate equation assumes that the total concentration of inhibitor added, [I], approximates to that free in solution. This approximation does not hold for some potent compounds, because there is depletion of free inhibitor by binding to the target enzyme. Such situations may be described by the rate equation for tight binding inhibition (*17*, *18*), which allows estimation of the value of an additional variable that is the concentration of binding sites. The concentration required for 50% inhibition (IC_{50}) is given by ($K_i' + [E_0]/2$) where $[E_0]$ is the concentration of binding sites. Eq 1 describes the situation where $K_i' \gg [E_0]$, and $IC_{50} \approx K_i'$. Tight binding occurs when $K_i' \approx [E_0]$. For more potent compounds, inhibition is stoichiometric ($K_i' \ll [E_0]$, and $IC_{50} \approx [E_0]/2$), again allowing estimation of the magnitude of $[E_0]$. These inhibitors lead to biphasic kinetics. In the first

phase, [I] ≤ [E_0], so that the measured rate decreases as an approximately linear function of [I]

$$v = k_p([E_0] - [I]) \quad (2)$$

where k_p is the rate of reaction per binding site. No further effect of increasing inhibitor concentration occurs ($v = 0$) during the second kinetic phase where [I] ≥ [E_0]. Analysis of stoichiometric kinetics, therefore, requires selection between two rate equations according to the relative values of [I] and [E_0]. Such a procedure was applied using *GraFit*.

Isothermal Titration Calorimetry. This was performed under the conditions employed for assay of EACPR activity in the absence of crotonoyl CoA, using an MCS titration calorimeter (MicroCal Inc., Northampton, MA) as described previously (*19*). EACPR (concentration of binding sites approximately 10−30 μM) was in the sample cell (volume 1.3449 mL) and NADH (300−450 μM) was added, typically as one injection of 2 μL, followed by 50−60 of 5 μL. Data were analyzed by fitting a simple, single-site model (*20*). Here, the calculated parameters of interest are K_d and the stoichiometry of binding, which reflects the proportion of the total protein that is functional. The total concentration of protein was estimated from the A_{280}, assuming $\epsilon = 14\,890$ M^{-1} cm^{-1}, which was calculated from the amino acid composition according to the formula of Mulvey et al. (*21*).

Gel Filtration Chromatography. PD10 columns (Pharmacia Biotech, Little Chalfont, Buckinghamshire, U. K.) were used in 50 mM sodium phosphate, pH 7.5, as described by the manufacturer. The manufacturers report that this procedure may remove over 96% of the low M_r material from protein solutions (measured using NaCl and human serum albumin).

Mass Spectrometry. Liquid Chromatography was performed on an HP1090 (Hewlett-Packard, Waldbrunn, Germany), followed by analysis on a BioQ Mass Spectrometer (Micromass, Manchester, U. K.). Samples were generated by incubating various combinations of enzyme, triclosan, and coenzymes for 30 min at room temperature. For measurement of triclosan, any reaction was stopped by addition of three volumes of acetonitrile. Samples then were resolved by isocratic liquid chromatography using 85% (v/v) acetonitrile in water on a Spherisorb C18 column (Waters, Milford, MA), of 4.6 mm diameter and 25 cm length. Triclosan was monitored in negative ion electrospray, using the three principal isotopic ions at m/z = 287, 289, and 291. For measurement of NAD^+, any reaction was stopped by addition of trifluoroacetic acid to 5% (v/v). Sample resolution was by isocratic liquid chromatography, using 10% (v/v) acetonitrile in water on a 4.6 mm by 25 cm ODS3 column (Phenomenex, Macclesfield, U. K.). NAD^+ was monitored in positive ion electrospray at m/z = 664.

Formation of any complexes between triclosan and NAD^+ also was investigated further in the samples used for measurement of NAD^+. The chromatography was changed to gradient elution with 10 to 95% (v/v) acetonitrile in water over 30 min from a 380 μm by 15 cm C18 base-deactivated silicon column (LC Packings, Amsterdam, Netherlands). A QToF Mass Spectrometer (Micromass, Manchester, U. K.) was used in positive and negative spectrum modes.

Characterization of Inhibition by Triclosan in the Steady-State. The rationale for this protocol is described in the Results section. Approximately 15 nM *E. coli* EACPR was preincubated with various concentrations of NADH, NAD^+ and triclosan for 5 h at 4 °C. The mixture (990 μL) was warmed to 25 °C and then 10 μL of crotonoyl CoA (final concentration 500 μM) was added in order to start the assay. This small change in volume had a minimal effect on the established equilibria. The maximum change in A_{340} during the assay corresponded to at most an 18% increase in NAD^+ concentration. Around 5% increase was typical. These experiments enabled application of eq 1 to estimate the value of the apparent inhibition constant, K_i', in the presence of different concentrations of coenzymes. The mechanism of inhibition was identified from the substrate dependence of K_i' (*22*) as follows. For pure noncompetitive kinetics, $K_i' = K_{is} = K_{ii}$, where K_{is} and K_{ii} are the inhibition constants for the slope and intercept terms on Lineweaver−Burk plots (*23*) and relate respectively to the affinity for inhibitor at zero and saturating concentrations of the varied substrate. The substrate dependence of K_i' for competitive, uncompetitive and mixed noncompetitive kinetics is shown in eqs *3*−*5*, respectively

$$K_i' = K_{is}([S] + K_m)/K_m \quad (3)$$

$$K_i' = K_{ii}([S] + K_m)/[S] \quad (4)$$

$$K_i' = K_{is}K_{ii}([S] + K_m)/(K_{is}[S] + K_{ii}K_m) \quad (5)$$

The *F*-test described above was used to assist in identification of the substrate dependence of K_i' and so the mechanism of inhibition.

Crystal Structure. EACPR/coenzyme/triclosan complexes crystallized in a variety of forms. The monoclinic form described in detail here was grown as follows. Hanging drops were formed by mixing 4 μL of complex solution (15 mg/mL protein, 3 mM NADH, 0.6 mM triclosan) with 4 μL of a reservoir solution, containing 12−16% (w/v) poly(ethylene glycol) 400 and 0.1 M sodium acetate (pH 4.8−5.2), at room temperature. The crystals obtained belong to space group $P2_1$, with cell dimensions a = 74.2 Å, b = 80.3 Å, c = 82.8 Å, β = 104.5°, and contain one tetramer in the asymmetric unit. A data set was collected from two crystals at room temperature at the SRS, Daresbury, UK (station 9.6; wavelength 0.87 Å). Data were processed using a version of MOSFLM modified for image plate data. The CCP4 suite of programs (*24*) was used for data reduction and subsequent data handling. The structure was solved using the molecular replacement program AMoRe (*24*), with a structure of a diazaborine complex as trial model. Averaged-difference ($F_{obs} - F_{calc}$) electron-density maps clearly showed the location of both the coenzyme and the triclosan. Isomorphous crystals were obtained with NAD^+ in the starting crystallization mixture and the resultant 3 Å structure is consistent with the structure described here. The location of triclosan also was confirmed in two other crystal forms. The coenzyme structure appears the same, regardless of whether the crystals are grown from mixtures initially containing NADH or NAD^+. These data suggest, but do not prove, that the bound coenzyme is NAD^+, which is consistent with the kinetic mechanism of inhibition by triclosan (see below) and with the limited stability of NADH at the pH used for crystallization. The structure was refined using the program XPLOR

Table 1: X-ray Data and Refinement Statistics

	overall	highest shell
resolution (Å)	53.45−1.90	2.00−1.90
no. measurements	92 854	5607
unique reflections	57 294	4320
completeness (%)	78.2	40.6
multiplicity	1.6	1.3
R_{merge} (%)	9.9	45.9
R_{factor} (%)	20.1	26.5
R_{free} (%)	20.7 (1717 reflections)	27.9
	deviations from ideality	
rms bond lengths (Å)	0.011	
rms bond angles (deg)	1.448	

(*25*). The refinement of atomic positions was alternated with the refinement of individual temperature factors, enforcing strict noncrystallographic symmetry and applying a bulk-solvent factor correction (*26*). Data collection and refinement statistics are shown in Table 1. The final coordinates have been deposited in the Protein Data Bank with accession code 1QG6.

RESULTS

Kinetic Characteristics of EACPR. Enoyl ACP is difficult to obtain in suitable quantities and purity for detailed kinetic studies. However, crotonoyl CoA (which also contains a thioester to phosphopantothene) is used as a model substrate (*2*−*4*). In the current study, a K_m value of (4.0 ± 0.6) mM is estimated for crotonoyl CoA in the presence of a fixed concentration of 100 μM NADH. This K_m value is similar those reported previously (*2*, *3*). The value of k_{cat} is calculated as (10 ± 1) s^{-1}, which is around 40-fold higher than a published estimate with crotonoyl CoA, and 2-fold higher than a reported figure for crotonoyl ACP (*3*). These differences may reflect a tendency for the kinetic properties of EACPR to change during isolation and storage (*4*). The current protocols aim to avoid this instability, and the enzyme preparations appear fully active (close to 1 mol NADH bound per mol EACPR monomer) and homogeneous in function (because a good fit is obtained using a simple single-site model) when characterized by isothermal titration calorimetry.

It is difficult to measure precisely the K_m for NADH because the change in A_{340} is small during assays at subsaturating concentrations. Approximate K_m values in the range 4.0 to 5.1 μM are obtained in the presence of 500 μM crotonoyl CoA and the absence of added NAD^+. The K_d value of NADH has been measured 11 times by isothermal titration calorimetry. Taking the logarithms of these values, averaging and then taking the antilogarithm gives an estimated $K_d = 5.4$ μM (95% confidence intervals 2.6 to 11 μM). The mean stoichiometry of binding is (0.91 ± 0.09) mol NADH/mol EACPR monomer, and the mean $\Delta H°$ is -(14.5 ± 1.6) kcal/mol. ($\Delta G° = -7.2$ kcal/mol, $T\Delta S° = -7.3$ kcal/mol.) A representative thermogram is shown in Figure 1. The agreement between the values of K_m in the presence of crotonoyl CoA and K_d in its absence are reasonable, especially since crotonoyl CoA is present at a fraction of its K_m value during the activity assays. During the subsequent studies, the apparent affinity of NADH in the presence of 500 μM crotonoyl CoA is taken as $K_m \approx K_d \approx 5.4$ μM.

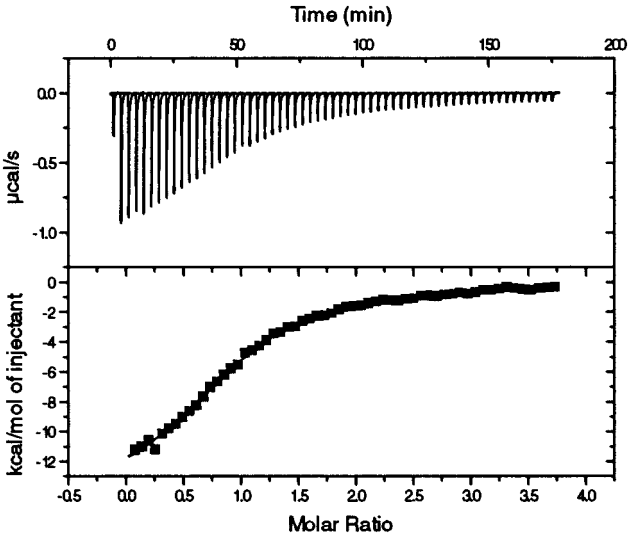

FIGURE 1: Isothermal titration calorimetry of EACPR and NADH. The initial concentration of EACPR subunits in the cell was 29 μM. NADH (450 μM) was added as one injection of 2 μL, followed by 58 of 5 μL. The best fit parameter values are $K_d = (7.8 \pm 0.9)$ μM, $\Delta H° = -(15.1 \pm 0.2)$ kcal/mol, and stoichiometry of (0.95 ± 0.01) mol NADH bound per mol EACPR subunits.

The affinity of NAD^+ for *E. coli* EACPR (dissociation constant, K_{NAD}) has been estimated by characterizing its action as a product inhibitor. NAD^+ follows competitive kinetics ($K_{is} = 1.9 \pm 0.3$ mM) with respect to NADH at 1400 μM crotonoyl CoA. A similar affinity is estimated from isothermal titration calorimetry when NADH displaces NAD^+ from EACPR in the absence of enoyl substrate. A mixture of EACPR and 20 mM NAD^+ in the calorimeter cell was titrated with NADH containing 20 mM NAD^+. The apparent K_d for NADH was increased due to competition by NAD^+ and was poorly defined at (66 ± 55) μM, because the $\Delta\Delta H°$ when NADH replaced bound NAD^+ was small (approximately −2.7 kcal/mol). These data lead to approximate estimates for NAD^+ having a $K_d = 1.8$ mM and $\Delta H° = -12$ kcal/mol ($\Delta G° = -3.7$ kcal/mol, $T\Delta S° = -8.1$ kcal/mol).

Triclosan is a Stoichiometric Inhibitor in the Potency Assay. Enzyme-catalyzed depletion of NADH was measured in the presence of various concentrations of triclosan. Initial studies were performed by estimating the rate from measurements of A_{340} made at the start of the assay and again 30 min later. A poor quality of fit is obtained when a standard relationship for enzyme inhibition (eq 1) is fitted to the estimated rates. Calculated IC_{50} values ($\approx$ 40 nM) are around 50% of the expected concentration of binding sites, suggesting that most of the added inhibitor is binding to EACPR. Accordingly, a rate equation for tight binding inhibition (*16*) was fitted to the measured rates. This leads to uncertainty in the estimated values of K_i', which appear to be smaller than the concentrations of binding sites. A relationship describing stoichiometric inhibition (eq 2), therefore, was fitted to the data. This equation assumes that all of the added inhibitor becomes bound to EACPR whenever the inhibitor concentration is below that of the binding sites. A good quality of fit is obtained (Figure 2). As expected for stoichiometric inhibition, the estimated concentration of sites varies as a linear function of the quantity of enzyme in the assay.

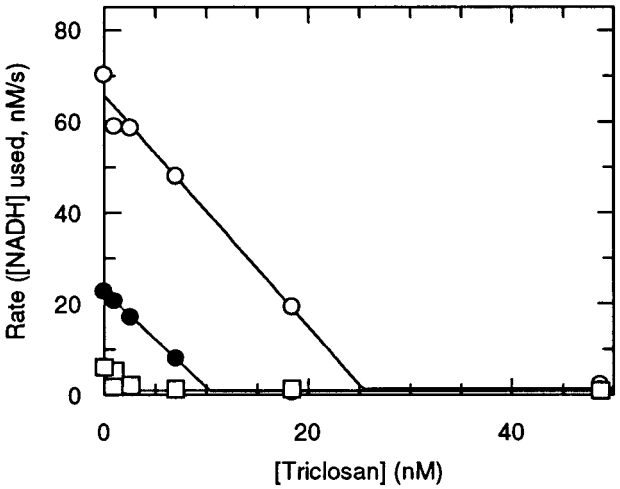

FIGURE 2: Inhibition of EACPR by triclosan in the potency assay. Assays were performed at different concentrations of enzyme. Fitting eq 2 to the data gives estimates of $[E_0]$ as □, (3.4 ± 0.3) nM; ●, (10 ± 0.1) nM; ○, (25 ± 1) nM. These values are close to those expected from dividing total protein concentration by subunit M_r.

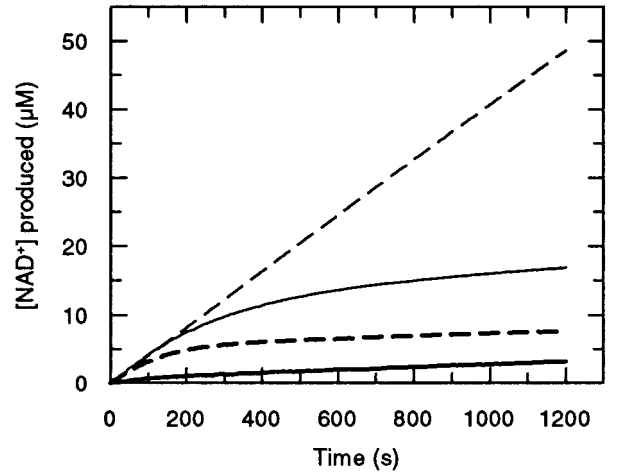

FIGURE 3: Slow onset of inhibition by triclosan. The following variations of the potency assay were used: dashed line, no NAD^+ or triclosan added, no preincubation; solid line, no NAD^+ added, 150 nM triclosan, no preincubation; heavy dashed line, 100 μM NAD^+ added, 150 nM triclosan, no preincubation; heavy solid line, 100 μM NAD^+ added, 150 nM triclosan, 30 min preincubation.

Inhibition by Triclosan is Promoted by Added NAD^+ and Preincubation with EACPR. The potency assay protocol involves preincubation of EACPR, NAD^+, and inhibitor, prior to starting the assay. Continuous measurement of A_{340} was used in order to investigate the consequences of omission of the preincubation and added NAD^+ (Figure 3). The accumulation of product is linear with time in the absence of preincubation, added NAD^+, or triclosan. Addition of 150 nM triclosan without preincubation leads to a gradual onset of inhibition. The onset of inhibition is more rapid when 100 μM NAD^+ also is added. The degree of inhibition is almost constant after preincubation for 30 min in the presence of 150 nM triclosan and 100 μM NAD^+.

Gel Filtration Shows that Inhibition of EACPR Activity is Reversible. The high potency of triclosan led us to question the reversibility of inhibition. To test reversibility, 0.5 μM EACPR was preincubated with various reagents for 30 min at room temperature prior to gel filtration chromatography in order to remove unbound low M_r components. Catalytic activity then was measured by diluting the enzyme to 25 nM in 100 μM NADH and 1 mM crotonoyl CoA. Similar rates are obtained after preincubation of enzyme alone, EACPR with 0.5 μM NAD^+, EACPR with 1 μM triclosan, or EACPR with 0.5 μM NADH and 1 μM triclosan. There is initially over 90% inhibition after preincubation of EACPR with 0.5 μM NAD^+ and 1 μM triclosan. This is followed by a gradual decrease in the degree of inhibition to around 75% after 30 min. These results indicate that binding of triclosan is strongest in the presence of NAD^+, and that inhibition is reversible in that functional enzyme is regenerated.

Mass Spectrometry Shows that Neither Triclosan, nor NAD^+, is Irreversibly Modified During Inhibition. The gel filtration experiments do not evaluate whether triclosan is consumed during inhibition, in a manner similar to diazaborines (*6*) and the isoniazid metabolite (*9*). An analogous mechanism to these potent inhibitors would lead to destruction of triclosan and NAD^+ and formation of one or more products. This possibility was investigated by mass spectrometry, which led to the following conclusions.

Following incubation under conditions where all of the triclosan is expected to be bound, 35% of the inhibitor is recovered, suggesting that irreversible formation of an adduct with NAD^+ is not required.

The fraction of triclosan recovered after incubation under conditions which lead to stoichiometric inhibition (see above) is similar to that recovered (33%) under conditions that are expected to give no binding (NAD^+ added after quenching).

The results are similar when monitoring stoichiometric NAD^+, rather than triclosan (98% recovery under inhibitory conditions, and 90% when NAD^+ added after quenching).

No new products can be detected after incubating triclosan and NAD^+ in the presence, or absence of EACPR, followed by quenching with either acetonitrile or trifluoroacetic acid.

Characterization of Inhibition by Triclosan in the Steady-State. These studies could not be performed using the potency assay because inhibition has a slow onset and becomes stoichiometric. A revised protocol was designed in order to satisfy the following conditions:

(1) An approximation to steady-state is reached before starting the assay and then maintained.

(2) The apparent affinity for triclosan is reduced to measurable levels (K_i' not $\ll [E_0]$), by inclusion of NADH at suitable concentrations to allow competition with the NAD^+ that is required for potent inhibition.

(3) The concentration of NAD^+ does not change significantly during the assay, so that the apparent affinity of triclosan remains constant.

Suitable protocols require preincubation of EACPR and triclosan in the presence of a low concentration of NAD^+ (relative to its apparent K_d) and a high concentration of NADH (relative to its apparent K_d). Under such conditions, only a small proportion of the enzyme may exist as the $E-NAD^+$ complex, which has a high affinity for triclosan. Accordingly, binding of the inhibitor is likely to be slow and the preincubation must be of sufficient duration to allow equilibration. To characterize the mechanism of inhibition, the rate of reaction must be sufficient to measure with reasonable precision in the presence of inhibitor. These considerations impose limitations on the choice of concentrations of reagents, so that all concentrations of NADH are at

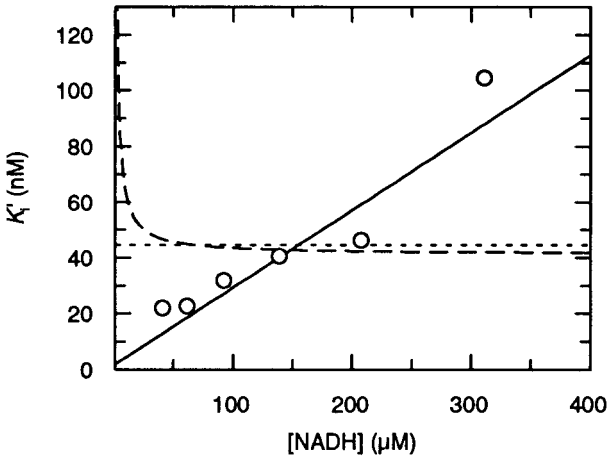

FIGURE 4: The effect of NADH on the apparent inhibition constant for triclosan. Best fit lines are shown for the following mechanisms of inhibition: Competitive (eq 3), solid line; uncompetitive (eq 4), long dashes; pure noncompetitive (eq 5, $K_{is} = K_{ii}$), short dashes. Only competitive inhibition gives an acceptable quality of fit, with $K_{is} = 1.5$ nM and $K_m = 5.4$ μM.

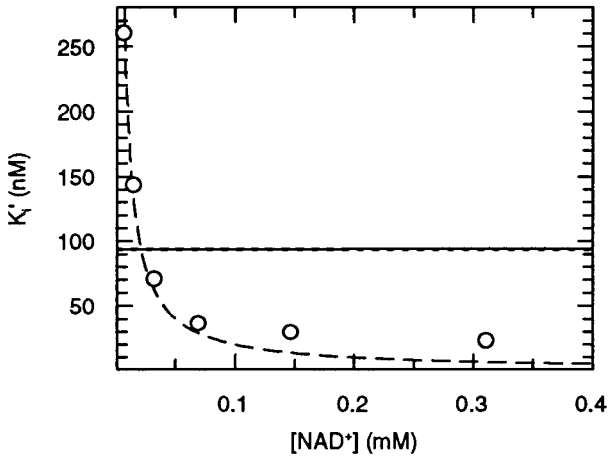

FIGURE 5: The effect of NAD^+ on the apparent inhibition constant for triclosan. Best fit lines are shown for the following mechanisms of inhibition: Competitive (eq 3), solid line; uncompetitive (eq 4), long dashes; pure noncompetitive (eq 5, $K_{is} = K_{ii}$), short dashes. Only uncompetitive inhibition gives an acceptable quality of fit, with $K_{ii} = 22$ pM and $K_m = 90$ mM.

least $7\times$ K_m, and all concentrations of NAD^+ are below $K_{NAD}/6$. These restrictions tend to make the fitted values of K_m and inhibition constants in eqs 3−5 dependent upon each other. Accordingly, the values of K_m were constrained to be equal to those obtained from independent studies, which were performed in the absence of triclosan.

(a) Triclosan Follows Competitive Kinetics with Respect to NADH. The values of K_i' for triclosan (eq 1) were measured in the presence of 50 μM NAD^+ at NADH concentrations between 42 and 310 μM using the protocol described above. The mechanism of inhibition was investigated by fitting eqs 3−5, with the value of K_m constrained to 5.4 μM because the concentration of NAD^+ was insufficient to have a competitive effect. The measured values of K_i' are consistent with competitive kinetics (eq 3), with $K_{is} = (1.5 \pm 0.1)$ nM at zero NADH. Equations for uncompetitive (eq 4) and pure noncompetitive inhibition (eq 5, $K_{is} = K_{ii}$) cannot describe accurately the observed relationship between K_i' and NADH concentration (Figure 4).

(b) Triclosan Follows Uncompetitive Kinetics with Respect to NAD^+. The values of K_i' for triclosan (eq 1) were estimated in the presence of 250 μM NADH at NAD^+ concentrations between 7.4 and 311 μM. The mechanism of inhibition was studied by fitting eqs 3−5, with the value of K_m for NAD^+ constrained to 90 mM. This value was calculated using eq 3, by taking the values of K_m for NADH as 5.4 μM, and K_{is} for NAD^+ as 1.9 mM. The measured values of K_i' are consistent with uncompetitive kinetics (eq 4), with $K_{ii} = (22 \pm 1)$ pM at saturating NAD^+. Expressions for competitive (eq 3) and pure noncompetitive inhibition (eq 5, $K_{is} = K_{ii}$) cannot describe accurately the observed relationship between K_i' and NAD^+ concentration (Figure 5).

(c) Interpretation of Steady-State Kinetics. The competitive kinetics with respect to NADH imply that prior binding of the reduced coenzyme decreases affinity for triclosan. The uncompetitive kinetics when NAD^+ is varied show that prior binding of the oxidized coenzyme promotes association of the inhibitor. Thus, these studies are consistent with each other in suggesting that the binding of triclosan is promoted by prior association of EACPR with NAD^+, and that NADH competes with the oxidized coenzyme (Scheme 1). (E−NADH is shown in brackets because K_m is a macroscopic constant, which reflects the dissociation of NADH from an unspecified number of intermediates.)

Scheme 1

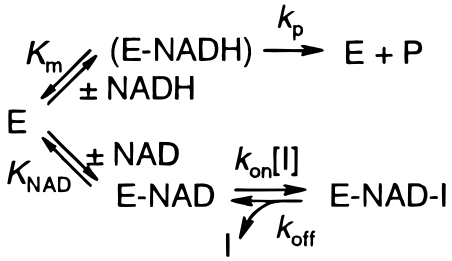

The Rate Constant for Dissociation of Triclosan. This was estimated in experiments where 4.5 μM enzyme was preincubated with 5 μM inhibitor and 2 mM NAD^+ for 30 min at 25 °C, prior to 200-fold dilution into competing NADH and crotonoyl CoA. The dissociation of triclosan was monitored by following enzyme activity during the initial part of the time-course when the concentrations of substrates and NAD^+ were relatively constant. The concentration of triclosan was selected as sufficient to give strong inhibition (in order to minimize changes in concentrations of substrates and products) and low enough to minimize association after dilution.

Rate equations for this system are derived in the Appendix. Data were analyzed by fitting an integrated rate equation (eq A15), which describes the amount of product formed as a function of time (Figure 6). Analysis of the full time-course was not possible because the concentrations of free inhibitor and NAD^+ did not approximate to constant values. To avoid a significant change in NAD^+ concentration, the assay time was limited to approximately 25% of the $t_{1/2}$ for regain of EACPR activity. This prevented accurate calculation of the steady-state rate, v_s, when eq A15 was fitted to the data. Accordingly, the value of v_s was constrained to equal the uninhibited rate. During the early part of the time-course, there was an approximation to no reassociation of triclosan because E−NAD^+ and free inhibitor were both at low concentrations, and there was competition by NADH and

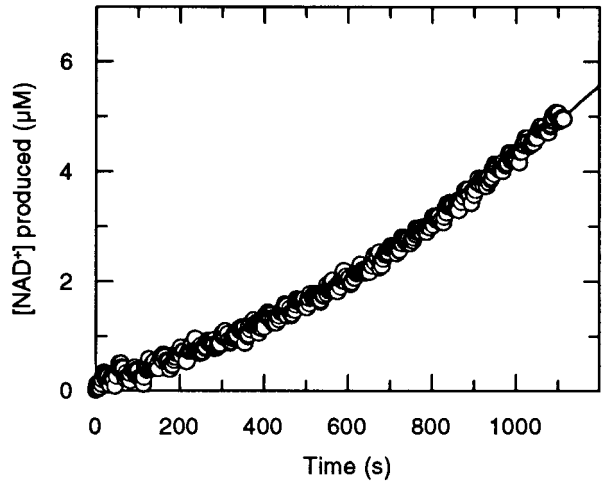

FIGURE 6: Formation of NAD^+ during dissociation of triclosan from EACPR. Enzyme was preincubated with triclosan and NAD^+, and then diluted into competing 200 μM NADH and 500 μM crotonoyl CoA. Data were analyzed by nonlinear regression of eq A15 with v_s constrained to 0.025 μM/s, which gave best fit values of $a = (1.87 \pm 0.03) \times 10^{-4}$ s^{-1} and $v_0 = (2.24 \pm 0.03) \times 10^{-3}$ μM/s. The best fit line is shown.

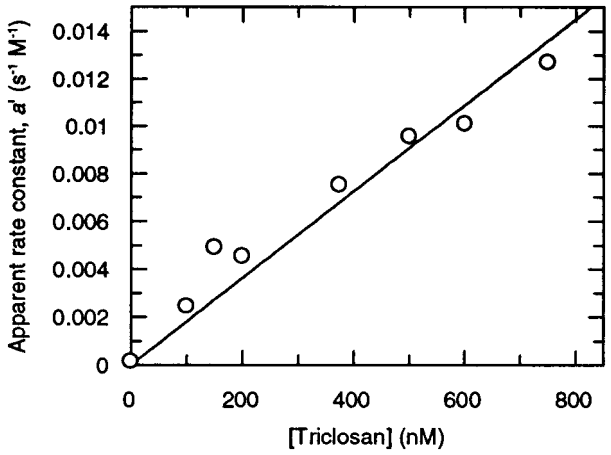

FIGURE 7: The rate constant for onset of inhibition at various triclosan concentrations. Assays were started by addition of enzyme to a mixture of NAD^+, substrates, and various concentrations of triclosan. Eq A15 was fitted to the observed accumulation of product in order to estimate values of the rate constant for onset of inhibition, a'. The value of a' at zero inhibitor is taken as that of k_{off} from experiments monitoring dissociation of triclosan. Eq A33 was fitted to the values of a', with k_{off} constrained to 1.9×10^{-4} s^{-1}. The gradient of the line that is shown is calculated from the best fit value $(1.81 \pm 0.09) \times 10^4$ s^{-1} M^{-1}, which corresponds to $(k_{on}K_i/K_i')$.

crotonoyl CoA. Accordingly, the apparent association rate constant, k_{on}', in eq A5 was much less than the dissociation rate constant, k_{off}. The calculated value of the apparent rate constant, a, in eq A15, therefore, was taken as an estimate of k_{off}. If the assumption of no significant reassociation was not valid, then the observed rate constant, a, would have been larger than k_{off} (see eq A5). Reassociation becomes greater at lower concentrations of competing NADH and crotonoyl CoA. Accordingly, the value of a was measured at a range of substrate concentrations in order to assess whether the minimum value had been obtained. In the presence of 20 to 200 μM NADH, and 500 to 1400 μM crotonoyl CoA, calculated values of a are between 1.0 and 2.8×10^{-4} s^{-1}. These data are consistent with a value of $k_{off} = 1.9 \times 10^{-4}$ s^{-1} (Figure 6).

The Rate Constant for Association of Triclosan. This was estimated in experiments where the onset of inhibition was monitored. The Appendix includes the derivation of equations, which describe the time-course of product accumulation in a system where inhibition requires prior binding of NAD^+ and is prevented by competing NADH (Scheme 1). Assays were started by addition of 20 nM enzyme to various concentrations of triclosan (100−750 nM), together with 200 μM NADH, 600 μM crotonoyl CoA and 50 μM NAD^+. Fitting of eq A15 allowed estimation of the values of the rate constant for onset of inhibition, a'. Eq A33 permits calculation of k_{on} and k_{off} from the observed values of a' at different concentrations of triclosan. However, all values of a' were $\gg k_{off}$, which limited the ability to estimate the value of k_{off}. Accordingly, during fitting of eq A33, the magnitude of k_{off} was constrained to that determined directly in dissociation studies (1.9×10^{-4} s^{-1}). The calculated gradient is $(1.8 \pm 0.1) \times 10^4$ s^{-1} M^{-1} (Figure 7), which corresponds to $(k_{on}K_i/K_i')$. The ratio K_i/K_i' was calculated as 1450 by rearrangement of eq A32, using $K_m = 5.4$ μM and $K_{NAD} = 1.9$ mM, so that $k_{on} = 2.6 \times 10^7$ s^{-1} M^{-1}.

Crystal Structure. In the present study, isomorphous monoclinic crystals containing triclosan have been grown in solutions that originally contained EACPR and either NADH, or NAD^+. The structures of the coenzyme in crystals obtained from NAD^+ or NADH could not be distinguished, although a higher resolution was obtained (1.9 compared to 3.0 Å) when the initial mixture contained reduced coenzyme. Each of these structures is similar to those recently obtained at 1.8 and 2.2 Å resolution from a hexagonal crystal form containing EACPR, coenzyme and triclosan (*12*, *28*). These characteristics suggest that NAD^+ is the coenzyme in crystals grown from mixtures that originally contained NADH, especially since triclosan has a higher affinity for the complex containing NAD^+, preparations of NADH often are contaminated with NAD^+, NADH is oxidized to NAD^+, and NADH is less stable than NAD^+ at the pH of crystallization.

In the 1.9 Å resolution structure presented here, triclosan is bound to EACPR and coenzyme (Figure 8) in a manner, which is reminiscent of that for the diazaborine compounds (*6*). The phenol(ate) ring of triclosan stacks directly over the nicotinamide ring of the coenzyme. Triclosan forms hydrogen bonds with the hydroxyl of Tyr-156 (2.6 Å) and with the nicotinamide ribose 2′-hydroxyl of the coenzyme (2.6 Å), which in turn hydrogen bonds (2.8 Å) to Lys-163 (Figure 8). One loop region (residues 196−205), which is disordered in the EACPR−NAD^+ complex (*6*), becomes ordered upon triclosan binding, and residues Thr-194 and Ala-196 interact with phosphate groups of the coenzyme. Conversely, this loop remains disordered in a recently published EACPR−coenzyme−triclosan complex (*28*). This difference appears to reflect triclosan being soaked into crystals (*28*), rather than cocrystallized with the protein (in the present study). It appears that binding of triclosan in solution causes increased order in the loop, which is preserved if the complex is crystallized. In the diazaborine complexes, residues 193−198 have high-temperature factors and do not interact with either the coenzyme or the inhibitor (*6*).

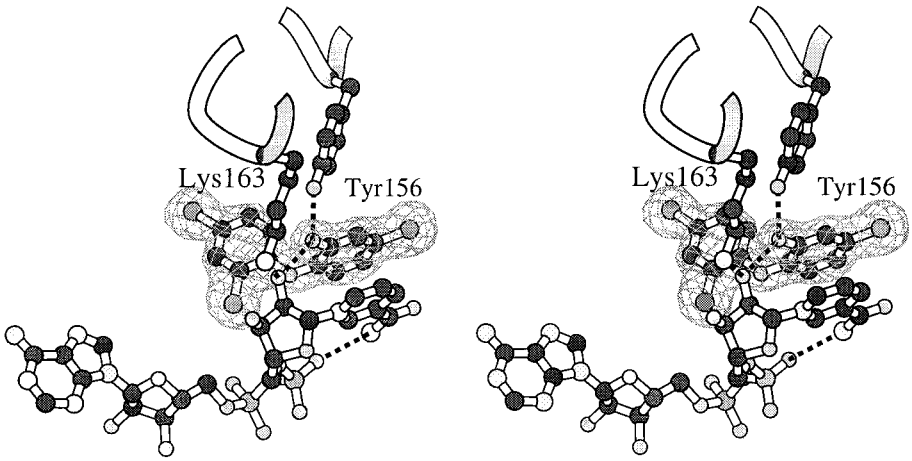

FIGURE 8: Defocused stereoview of the EACPR active site, with difference electron density for bound triclosan. The coenzyme, triclosan, and selected protein side-chains are shown in all-atom representation. Triclosan stacks on the nicotinamide ring of the cofactor, also forming a close contact with Tyr-156. Figure was generated using the program BOBSCRIPT (*27*).

DISCUSSION

Kinetic Characterizics of EACPR. Isothermal titration calorimetry demonstrates that NADH and NAD^+ bind competitively to free enzyme. When crotonoyl CoA is present at a fraction of its K_m value, kinetic studies confirm competition between the coenzymes and show that the K_m for NADH is similar to the K_d. These results are consistent with an ordered sequential mechanism where NADH binds before crotonoyl CoA. Such a mechanism also is supported by crystallographic data on EACPR (from *E. coli* and *B. napus*) and InhA protein from *M. tuberculosis* (*6*, *8*, *29*, *30*). Calorimetric and kinetic studies on the *M. tuberculosis* enzyme show that ordered sequential binding with NADH first is favored over random association of substrates (*5*).

Inhibition by Triclosan is Reversible and Appears to Require NAD^+. The preincubation with NAD^+ was included in the high throughput screen and subsequent potency assay because inhibition of EACPR by diazaborines was known to follow a slow onset, which involves formation of a covalent bond to the coenzyme in E−NAD^+ complex (*6*). Similar kinetics and cofactor dependence are exhibited by triclosan (Figure 3). Experiments where the concentrations of triclosan and EACPR are varied show that the compound can lead to stoichiometric inhibition (Figure 2). Such high affinity questions whether inhibition is reversible. In addition to the diazaborines, there is precedent for potent inhibition of EACPR and other redox enzymes, which involves formation of covalent bonds involving the inhibitor. Similar mechanisms are followed during inhibition of aldose reductase (*31*) and lactate dehydrogenase (*32*) by covalent complexes formed between substrate and bound oxidized coenzyme and during inhibition of *M. tuberculosis* InhA protein by an isoniazid metabolite (*9*). For InhA, aldose reductase and lactate dehydrogenase, an adduct is formed via C4 of the nicotinamide ring of the coenzyme, leading to an increase in ϵ_{340}. However, we find no change in absorbance spectra when EACPR is incubated with NAD^+ and triclosan, suggesting that an analogous covalent bond is not formed. This conclusion is reinforced by the crystal structure. Furthermore, following gel filtration and dilution into NADH and crotonoyl CoA, EACPR shows a gradual regain of catalytic activity after inhibition by triclosan in the presence of NAD^+. This result showed that any modification of the enzyme is reversible. Subsequent mass spectrometry suggests that neither triclosan nor NAD^+ is destroyed during inhibition of EACPR. The potent inhibition of EACPR by triclosan, therefore, follows a different mechanism to diazaborines and the isoniazid metabolite.

Kinetics of Inhibition. Enzyme inhibitors often are characterized using initial rate assays, which are started in the absence of product. This approach would not approximate to the steady-state in the presence of triclosan because accumulation of NAD^+ changes the rate of reaction. The degree of inhibition would increase during the assay (as observed in Figure 3) and triclosan would be less potent than in the presence of added NAD^+. These characteristics explain why an IC_{50} of 2 μM is seen for inhibition of *E. coli* EACPR by triclosan in the absence of exogenous NAD^+ (*11*).

Care is required during interpretation of the kinetics of inhibition. Competition by NADH (Figure 4) could suggest that triclosan binds at the same site as the coenzyme. Conversely, the uncompetitive kinetics when NAD^+ is varied (Figure 5) imply that association of the oxidized coenzyme increases the affinity for the inhibitor. Thus, it seems that the competition by NADH is an indirect result of its ability to prevent binding of NAD^+ and not due to a direct interaction at the same site as triclosan (Scheme 1). This mechanism is consistent with the gel filtration studies where inhibition after chromatography is detected only if NAD^+ is included in the preincubation with triclosan. Furthermore, crystallography shows that triclosan does not bind at the site for coenzyme (Figure 8). Given that binding of triclosan requires prior association with NAD^+, triclosan is likely to bind at the site for enoyl substrate. Displacement of triclosan by crotonoyl CoA is not significant over the <5 min timescale of the steady-state assays because the inhibitor dissociates slowly ($k_{off} = 1.9 \times 10^{-4}$ s^{-1}, $t_{1/2} = 61$ min) and the substrate is present at a fraction of its K_m value.

The steady-state experiments do not allow measurement of the affinity of triclosan for E−NADH complex, because it is much lower than that for E−NAD^+. The observed inhibition constant when NADH is varied ($K_{is} = 1.5$ nM) is higher than that in the study where NAD^+ concentrations are changed ($K_{ii} = 22$ pM). This difference appears to arise because the NAD^+ experiment estimates affinity at saturating levels of the oxidized coenzyme, whereas the NADH study

estimates affinity when NAD^+ is at 50 μM, which is a fraction of the estimated K_d = 1.9 mM. The inhibition constant at saturating NAD^+ can be predicted from the data when NADH is varied by rearranging eq 4, taking $K_i' = 1.5$ nM, $K_m = 1.9$ mM, and [S] = 50 μM. This approach gives an inhibition constant of 38 pM at saturating NAD^+, which is close to the $K_{ii} = 22$ pM when the oxidized coenzyme is varied. Furthermore, the pre-steady-state studies allow estimation of the K_d for triclosan as k_{off}/k_{on}, which gives 7.1 pM. Given the difficulties in characterizing a compound with the potency of triclosan, this value is in reasonable agreement with the inhibition constants from steady-state kinetics, supporting the validity of the different approaches used to estimate the affinity of this inhibitor.

The measured value of k_{on} (2.6×10^7 s^{-1} M^{-1}) is less than 100-fold below the diffusion controlled maximum (*33*) and could lead to the onset of inhibition having a $t_{1/2}$ of 2.6 s at 10 nM triclosan. The observed onset of inhibition is much slower (in Figure 7, the apparent rate constant is 1.8×10^4 s^{-1} M^{-1}), because triclosan associates primarily with E−NAD^+ complex, which appears to be only a minor fraction of the total enzyme under the conditions of the assay.

There are further consistencies in the kinetic studies. The v_s values from onset of inhibition at different triclosan concentrations can be analyzed by fitting eq 1. After correction for competition by NADH and uncompetitive kinetics with respect to NAD^+ (eq A32), this approach gives an estimate of $K_i \approx 24$ pM. Furthermore, eq A32 allows prediction of an apparent inhibition constant, K_i', of 2−10 nM under the conditions of the potency assay. This is consistent with the observation of stoichiometric inhibition, which gives estimates of concentrations of binding sites between 3.4 and 25 nM (Figure 2).

Triclosan Appears to be an Analogue of an Intermediate in Catalysis. On the basis of the crystal structure of a complex between *B. napus* EACPR, and NAD^+, Rafferty et al. (*29*) proposed a catalytic mechanism involving an enolate intermediate, which accepts a proton from the hydroxyl of Tyr-156 (*E. coli* numbering). C3 of the substrate is thought to be the subject of hydride attack by NADH. X-ray studies on crystals containing coenzyme, triclosan, and *E. coli* EACPR (*12*, *28*, and Figure 8) show that the inhibitor occupies the same site as diazaborines and the isoniazid metabolite (*6*, *7*, *9*). In these structures, triclosan may be ionized to give the phenolate (pK_a = 7.9, ref *34*), which appears to mimic the enolate of the proposed intermediate. It forms short hydrogen bonds (2.6 Å) with the hydroxyl of Tyr-156 and the nicotinamide ribose 2′-hydroxyl of the coenzyme (Figure 8). The crystal structures of *E. coli* EACPR in complex with NAD^+ and either thienodiazaborine or benzodiazaborine reveal that a covalent bond is formed between the inhibitor and the coenzyme (*6*). In contrast, there is no covalent attachment of triclosan to the cofactor, or to the enzyme (Figure 8 and refs *12*, *28*). This is consistent with the mass spectrometry and the reversible nature of inhibition. In the crystal structure, the phenol(ate) ring of triclosan stacks above the nicotinamide ring of the coenzyme, which is positively charged for NAD^+, raising the possibility of a charge-transfer effect, which may contribute to affinity. This may increase the preference for enzyme-bound NAD^+ over NADH in the complex with the inhibitor. The C5−C6 bond in the phenolic ring of triclosan seems to be in the position expected for the C2═C3 double bond of the enolate intermediate, with the 2,4-dichlorophenoxy moiety of triclosan being located in the region anticipated to bind the phosphopantothene of ACP (Figure 8 and ref *12*).

The 3-D structure suggests that the hydroxyl group of triclosan makes an important contribution to affinity. This hypothesis is supported by our observation that, at the limit of its solubility (100 μM), the *des*-hydroxyl analogue of triclosan leads to less than 21% inhibition in the potency assay. Thus, replacement of −OH by −H decreases affinity by more than 10 000-fold. The multiple hydrogen bonds made by the phenol(ate) of triclosan may be important in this contribution to binding. Further interactions may be associated with smaller entropic penalties having paid the entropic penalty for formation of one bond, so that the enthalpic gain from formation of subsequent bonds is seen as a larger contribution to the free energy of binding. Thus, the degree of enthalpy−entropy compensation (*35*) may be higher for the first bond, than for subsequent bonds, rather like the chelate effect (*36*). This rationale is consistent with other examples where hydroxyl groups make two hydrogen bonds and large contributions to affinity. Such a hydroxyl appears to increase the affinity by over 10^5-fold for 6-hydroxy-1,6-dihydropurine ribonucleoside binding to adenosine deaminase (*37*, *38*) and for Tyr binding to tyrosyl tRNA synthetase (*39*, *40*).

Biological Activity of Triclosan. The concentrations of NAD^+ and NADH in bacteria are respectively around 0.8 and 0.02 mM (*41*). Eq A32 predicts that the value of K_i' under these conditions is 0.1−0.6 nM. In assays following the effect of triclosan on the growth of *E. coli*, the minimum inhibitory concentration is 400 nM. Part of this change in potency upon moving to bacteria appears to reflect active pumping out of the cell, because deletion of the multidrug efflux pump locus, *acrAB*, increases sensitivity by approximately10-fold (*42*). Furthermore, the present study suggests that enoyl- and acyl-ACP may compete with triclosan for the binding site on EACPR. The high affinity of triclosan and its slow rate of dissociation contribute to its potency and duration of action (*43*) as an antibacterial agent.

ACKNOWLEDGMENT

We thank the following for their advice and contributions: A. R. Stuitje (provision of the clone expressing EACPR), D. W. Rice (sharing structural information prior to publication), C. Abell, J. Y. Beveridge, E. D. Clarke, J. M. Clough, M. I. Haigh, T. R. Hawkes, G. B. Hill, P. W. A. Howe, A. J. Pilgrim, N. F. Schnell, A. Wookey, and R. C. Viner.

APPENDIX: KINETIC ANALYSIS OF DISSOCIATION AND ASSOCIATION OF TRICLOSAN

Regain of Enzyme Activity due to Dissociation of Inhibitor. This is described in Scheme A1, where E−NAD corresponds to all forms of the enzyme with no bound inhibitor. Catalytic activity, therefore, is a function of [E−NAD]. The apparent rate constant for association of the inhibitor is k_{on}', which is a function of the microscopic association constant (k_{on}), [NAD^+], [NADH], K_{NAD}, and K_m. The rate of regain of catalytic activity is given by

Scheme A1

$$\text{E-NAD-I} \underset{k_{on}'[I]}{\overset{k_{off}}{\rightleftharpoons}} \text{E-NAD}$$

$$\frac{d[\text{E}-\text{NAD}]}{dt} = k_{off}[\text{E}-\text{NAD}-\text{I}] - k_{on}'[\text{I}][\text{E}-\text{NAD}] \quad \text{(A1)}$$

By conservation of mass, the total concentration of enzyme $[E_0]$, is given by

$$[E_0] = [\text{E}-\text{NAD}] + [\text{E}-\text{NAD}-\text{I}] \quad \text{(A2)}$$

$$\therefore \frac{d[\text{E}-\text{NAD}]}{dt} = k_{off}[E_0] - [\text{E}-\text{NAD}](k_{on}'[\text{I}] + k_{off}) \quad \text{(A3)}$$

$$= b - a[\text{E}-\text{NAD}] \quad \text{(A4)}$$

where

$$a = (k_{on}'[\text{I}] + k_{off}) \quad \text{(A5)}$$

and $b = k_{off}[E_0]$. Eq A4 rearranges to

$$dt = d[\text{E}-\text{NAD}]/(b - a[\text{E}-\text{NAD}]) \quad \text{(A6)}$$

Integration of this standard form (*44*) gives

$$t + c = (-1/a)\ln(b - a[\text{E}-\text{NAD}]) \quad \text{(A7)}$$

where c is the constant of integration. When $t = 0$, $[\text{E}-\text{NAD}] = [\text{E}-\text{NAD}]_0$

$$\therefore c = (-1/a)\ln(b - a[\text{E}-\text{NAD}]_0) \quad \text{(A8)}$$

Substituting into eq (A7) and rearranging

$$-at = \ln\left(\frac{(b/a) - [\text{E}-\text{NAD}]}{(b/a) - [\text{E}-\text{NAD}]_0}\right) \quad \text{(A9)}$$

At steady state, $d[\text{E}-\text{NAD}]/dt = 0$ and $[\text{E}-\text{NAD}] = [\text{E}-\text{NAD}]_s$. Substitution into eq A4 and rearrangement gives $[\text{E}-\text{NAD}]_s = b/a$, so that eq (A9) becomes

$$-\text{at} = \ln\left(\frac{[\text{E}-\text{NAD}]_s - [\text{E}-\text{NAD}]}{[\text{E}-\text{NAD}]_s - [\text{E}-\text{NAD}]_0}\right) \quad \text{(A10)}$$

Rate of reaction is given by $v = k_p'[\text{E}-\text{NAD}]$, where k_p' is an apparent constant. Thus,

$$-at = \ln\left(\frac{v_s - v}{v_s - v_0}\right) \quad \text{(A11)}$$

where the subscripts s and 0 relate respectively to steady and initial states. Eq A11 gives

$$v = v_s + (v_0 - v_s)e^{-at} \quad \text{(A12)}$$

Rate is $d[\text{P}]/dt$, so that

$$\int d[\text{P}] = v_s\int dt + (v_0 - v_s)\int e^{-at}\,dt \quad \text{(A13)}$$

$$\therefore [\text{P}] = v_s t - \left(\frac{v_0 - v_s}{a}\right)e^{-at} + c' \quad \text{(A14)}$$

When $t = 0$, $[\text{P}] = 0$, so that $c' = (v_0 - v_s)/a$

$$\therefore [\text{P}] = v_s t + (v_0 - v_s)(1 - e^{-at})/a \quad \text{(A15)}$$

So that a (defined in eq A5) is the apparent rate constant for regain of activity. Eq A15 is analogous to that derived by Morrison and Walsh (*45*) for a different mechanism, that is the transition from initial to steady state during slow binding inhibition. The present derivation is required in order to explain the magnitudes of v_0, v_s, and a when triclosan dissociates from EACPR.

Onset of Inhibition When Assays are Started by Addition of Enzyme. Scheme 1 shows the proposed kinetic scheme for inhibition by triclosan. The enzyme initially partitions between E, E−NAD, and E−NADH. At steady state, E−NAD−I also exists. During the shift from initial to steady state

$$\frac{d}{dt}([\text{E}] + [\text{E}-\text{NADH}] + [\text{E}-\text{NAD}]) = -k_{on}[\text{I}][\text{E}-\text{NAD}] + k_{off}[\text{E}-\text{NAD}-\text{I}] \quad \text{(A16)}$$

By definition, $K_m = [\text{E}][\text{NADH}]/\sum[\text{E}-\text{NADH}]$, where $\sum[\text{E}-\text{NADH}]$ represents all enzyme species after binding of NADH (*33*). Experimental data on the current system show that $K_m \approx K_d$ for NADH, so that $K_m \approx [\text{E}][\text{NADH}]/[\text{E}-\text{NADH}]$. Similarly, the inhibition constant for NAD^+ is $K_{is} = [\text{E}][\text{NAD}]/\sum[\text{E}-\text{NAD}]$. It is assumed that $K_{is} \approx K_{NAD} = [\text{E}][\text{NAD}]/[\text{E}-\text{NAD}]$, because concentrations of the reduced acyl-CoA product, butyryl CoA, are low (<7 μM), and it has a low affinity for EACPR (no inhibition is seen at 5 mM). Accordingly,

$$[\text{E}] = [\text{E}-\text{NADH}]K_m/[\text{NADH}] \quad \text{(A17)}$$

$$[\text{E}-\text{NAD}] = [\text{E}-\text{NADH}](K_m/[\text{NADH}])([\text{NAD}]/K_{NAD}) \quad \text{(A18)}$$

Substituting into eq A16, using [E] from eq A17 and [E−NAD] from eq A18 and then rearranging,

$$[\text{E}-\text{NAD}-\text{I}] = \frac{d}{dt}[\text{E}-\text{NADH}]\,\frac{1}{k_{off}}[1 + (K_m/[\text{NADH}])(1 + ([\text{NAD}]/K_{NAD}))] + \frac{k_{on}}{k_{off}}[\text{I}][\text{E}-\text{NADH}](K_m/[\text{NADH}])([\text{NAD}]/K_{NAD}) \quad \text{(A19)}$$

By conservation of mass, the total concentration of enzyme is given by

$$[E_0] = [\text{E}] + [\text{E}-\text{NADH}] + [\text{E}-\text{NAD}] + [\text{E}-\text{NAD}-\text{I}] \quad \text{(A20)}$$

Substituting into eq A20, using [E] from eq A17, [E−NAD] from eq A18, and [E−NAD−I] from eq A19, and then rearranging

$$\therefore \frac{d}{dt}[\text{E}-\text{NADH}] = b' - a'[\text{E}-\text{NADH}] \quad \text{(A21)}$$

where

$$b' = k_{off}[E_0]/[1 + (K_m/[NADH])(1 + ([NAD]/K_{NAD}))] \quad (A22)$$

$$a' = k_{off} + \left[\frac{k_{on}[I]([NAD]/K_{NAD})}{1 + ([NADH]/K_m) + ([NAD]/K_{NAD})}\right] \quad (A23)$$

Eq A21 is analogous to eq A4, so that rearrangement and integration gives

$$t + c'' = -(-1/a')\ln(b' - a'[E-NADH]) \quad (A24)$$

where c'' is the constant of integration. When $t = 0$, NAD^+ behaves as a competitive inhibitor with respect to NADH, so that the equilibrium method of Segel (*46*) gives

$$[E-NADH] = \frac{[E_0][NADH]}{K_m(1 + ([NAD]/K_{NAD})) + [NADH]} \quad (A25)$$

Substituting into eq (A24)

$$c'' = -\frac{1}{a'}\ln\left[b' - \frac{a'[E_0][NADH]}{K_m(1 + ([NAD]/K_{NAD})) + [NADH]}\right] \quad (A26)$$

Substituting into eq (A24) and rearranging

$$-a't = \ln\left[\frac{(b'/a' - [E-NADH])}{b'/a' - \frac{[E_0][NADH]}{K_m(1 + ([NAD]/K_{NAD})) + [NADH]}}\right] \quad (A27)$$

At steady state, $d[E-NADH]/dt = 0$ and eq A21 gives $[E-NADH]_s = b'/a'$, so that eq A27 becomes

$$-a't = \ln\left[\frac{([E-NADH]_s - [E-NADH])}{[E-NADH]_s - \frac{[E_0][NADH]}{K_m(1 + ([NAD]/K_{NAD})) + [NADH]}}\right] \quad (A28)$$

The rate of reaction, $v = k_p[E-NADH]$, so that eq A28 becomes analogous to eq A11. Thus, the kinetics for onset of inhibition follow eq A15, where the magnitude of a is given by that of a' in eq A23. The kinetics of onset of inhibition by triclosan, therefore, are similar to those derived by Morrison and Walsh (*45*) for different systems where there is slow isomerization of E−I complex. The present derivation is required in order to explain the magnitudes of v_0, v_s, and a' when triclosan associates with EACPR. These parameters are different to those in the system of Morrison and Walsh (*45*). Relationships describing v_0 and v_s can be derived by the equilibrium method of Segel (*46*), which gives

$$v_0 = \frac{V_{max}[NADH]}{K_m(1 + ([NAD]/K_{NAD})) + [NADH]} \quad (A29)$$

$$v_s = \frac{V_m[NADH]}{[NADH] + K_m(1 + ([NAD]/K_{NAD}) + ([NAD]/K_{NAD})([I]/K_i))} \quad (A30)$$

$$\therefore v_s = \frac{v_u}{1 + ([I]/K_i')} \quad (A31)$$

where v_u is the unihibited rate. K_i and K_i' are respectively the absolute and apparent inhibition constants for triclosan. K_i' is given by

$$K_i' = K_i[1 + (K_{NAD}/[NAD])(1 + ([NADH]/K_m))] \quad (A32)$$

The concentrations of NAD^+ and NADH are approximately constant, so that eqs A23 and A32 can be combined to give

$$a' = k_{off} + [I]k_{on}(K_i/K_i') \quad (A33)$$

REFERENCES

1. McCarthy, A. D., and Hardie, D. G. (1984) *Trends Biochem. Sci. 9*, 60−63.
2. Weeks, G., and Wakil, S. J. (1968) *J. Biol. Chem. 243*, 1180−1189.
3. Bergler, H., Wallner, P., Ebeling, A., Leitinger, B., Fuchsbichler, S., Aschauer, H., Kollens, G., Högenauer, G., and Turnowsky, F. (1994) *J. Biol. Chem. 269*, 5493−5496.
4. Bergler, H., Fuchsbichler, S., Högenauer, G., and Turnowsky, F. (1996) *Eur. J. Biochem. 242*, 689−694.
5. Quémard, A., Sacchettini, J. C., Dessen, A., Vilcheze, C., Bittman, R., Jacobs, W. R., Jr., and Blanchard, J. S. (1995) *Biochemistry 34*, 8235−8241.
6. Baldock, C., Rafferty, J. B., Sedelnikova, S. E., Baker, P. J., Stuitje, A. R., Slabas, A. R., Hawkes, T. R., and Rice, D. W. (1996) *Science 274*, 2107−2110.
7. Baldock, C., de Boer, G.-J., Rafferty, J. B., Stuitje, A. R., and Rice, D. W. (1998) *Biochem. Pharamacol. 55*, 1541−1549.
8. Dessen, A., Quémard, A., Blanchard, J. S., Jacobs, W. R., Jr., and Sacchettini, J. C. (1995) *Science 267*, 1638−1641.
9. Rozwarski, D. A., Grant, G. A., Barton, D. H. R., Jacobs, W. R., Jr., and Sacchettini, J. C. (1998) *Science 279*, 98−102.
10. McMurry, L. M., Oethinger, M., and Levy, S. B. (1998) *Nature 394*, 531−532.
11. Heath, R. J., Yu, Y.-T., Shapiro, M. A., Olson, E., and Rock, C. O. (1998) *J. Biol. Chem. 273*, 30316−30320.
12. Levy, C. W., Roujeinikova, A., Sedelnikova, S., Baker, P. J., Stuitje, A. R., Slabas, A. R., Rice, D. W., and Rafferty, J. B. (1999) *Nature 398*, 383−384.
13. De Boer, G.-J., Pielage, J. A., Nijkamp, H. J. J., Slabas, A. R., Raffery, J. B., Baldock, C., Rice, D. W., and Stuitje, A. R. (1999) *Mol. Microbiol. 31*, 443−450.
14. Leatherbarrow, R. J. (1996) *GraFit* (Version 3.09b) Erithacus Software, Staines, U. K..
15. Mannervik, B. (1982) *Methods Enzymol. 87*, 370−390.
16. Ward, W. H. J., Holdgate, G. A., Freeman, S. McTaggart, F., Girdwood, P. A., Davidson, R. G., Mallion, K. B., Brown, G. R., and Eakin, M. A. (1996) *Biochem. Pharmacol. 51*, 1489−1501.
17. Goldstein, A. (1944) *J. Gen. Physiol. 27*, 529−580.
18. Williams, J. W. and Morrison, J. F. (1979) *Methods Enzymol. 63*, 437−467.
19. Holdgate, G. A., Tunnicliffe, A., Ward, W. H. J., Weston, S. A., Rosenbrock, G., Barth, P. T., Taylor, I. W. F., Pauptit, R. A., and Timms, D. (1997) *Biochemistry 36*, 9663−9673.
20. Wiseman, T., Williston, S., Brandts, J. F., and Lin, L.-N. (1989) *Anal. Biochem. 179*, 131−137.
21. Mulvey, R. S., Gualtieri, R. J. and Beychok, S. (1974) *Biochemistry 13*, 782−787.
22. Cheng, Y.-C., and Prusoff, W. H. (1973) *Biochem. Pharmacol. 22*, 3099−3108.

23. Cleland, W. W. (1963) *Biochim. Biophys. Acta 67*, 173−187.
24. CCP4 (1994) *Acta Crystallogr. D50*, 760−763.
25. Brünger, A. T., Kuriyan, J., and Karplus, M. (1987) *Science 235*, 458−460.
26. Jiang, J.-S., and Brünger, A. T. (1994) *J. Mol. Biol. 243*, 100−115.
27. Esnouf, R. M. (1997) *J. Mol. Graphics 15*, 133−138.
28. Heath, R. J., Rubin, J. R., Holland, D. R., Zhang, E., Snow, M. E., and Rock, C. O. (1999) *J. Biol. Chem. 274*, 11110−11114.
29. Rafferty, J. B., Simon, J. W., Baldock, C., Artymiuk, P. J., Baker, P. J., Stuitje, A. R., Slabas, A. R., and Rice, D. W. (1995) *Structure 3*, 927−938.
30. Baldock, C., Rafferty, J. B., Stuitje, A. R., Slabas, A. R., and Rice, D. W. (1998) *J. Mol. Biol. 284*, 1529−1546.
31. Grimshaw, C. E., Shahbaz, M., and Putney, C. G. (1990) *Biochemistry 29*, 9936−9946.
32. Arnold, L. J., and Kaplan, N. O. (1974) *J. Biol. Chem. 249*, 652−655.
33. Fersht, A. R. (1985) in *Enzyme Structure and Mechanism*, 2nd ed., pp 104−105 and pp 150−152 W. H. Freeman and Company, New York.
34. Budavari, S. (1996) (Editor) in *The Merck Index*, 12th ed., p 9786, Merck Research Laboratories, Whitehouse Station, NJ.
35. Dunitz, J. D. (1995) *Chem. Biol. 2*, 709−712.
36. Jencks, W. P. (1981) *Proc. Natl. Acad. Sci. U.S.A.* 78, 4046−4050.
37. Wolfenden, R., and Kati, W. M. (1991) *Acc. Chem. Res. 24*, 209−215.
38. Wilson, D. K., Rudolph, F. B., and Quiocho, F. A. (1991) *Science 252*, 1278−1284.
39. Fersht, A. R., Shi, J.-P., Knill-Jones, J., Lowe, D. M., Wilkinson, A. J., Blow, D. M., Brick, P., Carter, P., Waye, M. M. Y., and Winter, G. (1985) *Nature 314*, 235−238.
40. Brick, P., Bhat, T. N., and Blow, D. M. (1989) *J. Mol. Biol. 208*, 83−98.
41. Penfound, T., and Foster, T. W. (1996) in *Escherichia coli and Salmonella typhimurium − Cellular and Molecular Biology*, 2nd ed.; (Neidhardt, F. C., Ed.) p 721, ASM Press, Washington, DC.
42. McMurry, L. M., Oethinger, M., and Levy, S. B. (1998) *FEMS Microbiol. Lett. 166*, 305−309.
43. Jenkins, S., Addy, M., and Newcombe, R. (1991) *J. Clin. Peridontol. 18*, 140−144.
44. Weast, R. C. (1986) (Editor in Chief) in *CRC Handbook of Chemistry and Physics* p A-21, CRC Press Inc, Boca Raton, Florida, 1986.
45. Morrison, J. F., and Walsh, C. T. (1988) *Adv. Enzymol. 61*, 201−301.
46. Segel, I. H. (1975) in *Enzyme Kinetics. Behavior and Analysis of Rapid Equilibrium and Steady-State Enzyme Systems* pp 22−24, John Wiley and Sons, New York.

BI9907779